

Experimental evidence of interface resonance states in single-crystal magnetic tunnel junctions

P.-J. Zermatten, G. Gaudin, G. Maris, M. Miron, and A. Schuhl

SPINTEC, URA2512 CEA-CNRS, INAC 1005 Building, 17 rue des Martyrs, 38054 Grenoble Cedex 9, France

C. Tiusan, F. Greullet, and M. Hehn

*Laboratoire de Physique des Matériaux, UMR7556, CNRS-Nancy Université, Boulevard des Aiguillettes, BP239,**54506 Vandoeuvre-lès-Nancy Cedex, France*

(Received 2 June 2008; published 2 July 2008)

All solid-state tunnel spectroscopy experiments performed on single-crystal Fe/MgO/Fe magnetic tunnel junctions show sharp features at 0.2 and 1.1 V. These peaks are observed on the electrical differential conductivity only in the antiparallel magnetic configuration and only for the voltage sign corresponding to the injection of electrons toward the bottom electrode. They are attributed to the conductivity of two different resonant states of the Fe(001)/MgO bottom interface. The analysis of the attenuation of these peaks as a function of the insulator thickness provides information on their symmetry.

DOI: [10.1103/PhysRevB.78.033301](https://doi.org/10.1103/PhysRevB.78.033301)

PACS number(s): 73.40.Gk, 73.40.Rw, 81.15.Hi

Nowadays, magnetic tunnel junctions (MTJs) benefit on a strong scientific interest¹ motivated both by their high potential for applications in sensor and storage devices and by the complex fundamental physics of spin dependent tunneling. Theoretical models of tunneling in single-crystal devices²⁻⁴ have been successfully confronted to experimental observations of giant high tunneling magnetoresistance (TMR) in single-crystal MTJs involving MgO tunnel barrier.⁵⁻⁸ In these systems, the large TMR effects are determined by the different tunneling mechanisms and symmetry-related decay rates of the Bloch waves for the majority- and the minority-spin channels within the barrier. According to Butler's theory,² along the $k_{\parallel}=0$ propagation direction, the transport properties of an epitaxial Fe/MgO/Fe stack are governed by the Δ_i symmetry bulk density of states (DOS) of the Fe electrodes and their different decay rates into the barrier. For the parallel configuration the transport is governed by the majority Δ_1 states which have the lowest decay rate into the barrier. For the antiparallel configuration, there are no Δ_1 states available at the Fermi level, the conductance being dominated by the Δ_5 states. Moreover, the electronic properties at the metal/barrier interface have been often proven to be important in determining the TMR sign and amplitude.⁹⁻¹¹ Surface states may appear at the ferromagnet/insulator interface through the breakdown of the translational symmetry.^{12,13} When coupled to the bulk, they become interfacial resonant states (IRSs) and are predicted to strongly affect and even dominate the tunnel transmission.^{2,4,14-16}

Experimentally, the surface states have been already studied for the Fe(001)/vacuum system below¹⁷ and above¹⁸ the Fermi level. However, at the Fe(001)/MgO interface, the nature of the interfacial electronic structure and its role on the spin dependent transport through the MgO barrier are expected to be more complex. Even in a perfect system, the chemical bondings at the Fe/MgO interface affect the Fe(001) electronic structure and modify the propagation by tunneling of existent IRS. Moreover, the cubic symmetry of the insulator will determine the tunneling attenuation of the IRS as a function of its symmetry. A direct analysis of the Fe(001) surface states covered by MgO above and under the Fermi level (E_F) is difficult by standard scanning tunneling

spectroscopy (unoccupied states) or photoemission experiments (occupied states). Attenuation by the MgO of the electron flow limits the analysis to low MgO thicknesses (few atomic planes) far from 2 to 3 nm MgO thickness in standard MTJs. Additional experimental difficulties to observe these resonant states are due to their quenching by roughness-related disorder.¹⁹ However, contribution of the minority-spin IRS on the tunneling transport¹¹ has been reported in model Fe(001)/MgO(001)/Fe(001) MTJ systems with low roughness level. In these experiments, the observed IRS is the one located at 0.2 eV above E_F . The question remains opened concerning the IRS at the top interface. Around 0.2 eV, the signature of the IRS is mixed with the one related to the top of the bulk majority-spin Δ_5 symmetry band which also affects the conductance.

In this Brief Report, we show direct experimental evidences of two minority interface resonant states in Fe/MgO/Fe tunnel junction at 0.2 and 1.1 eV. Our all solid-state tunneling spectroscopic observation is done through spin dependent transport measurements. Therefore, by varying the voltage sign during the tunneling spectroscopy experiments, we investigate separately the surface electronic structure of both the bottom and the top Fe/MgO interfaces. Our experiments show that these interfaces are asymmetric, a larger roughness at the top interface being responsible on the quenching of the IRS at the top interface.

The Fe/MgO/Fe/Co multilayer is grown by molecular beam epitaxy, as detailed in a previous work.²⁰ Briefly, after annealing the MgO substrate at 500 °C for 20 min, a first 45-nm-thick Fe layer is deposited at room temperature using a Knudsen cell, then annealed at 450 °C for 15 min in order to smooth its surface. The MgO insulating layer is subsequently deposited at room temperature using an electron gun. With a shutter we defined three different MgO areas with thicknesses of 2.2, 2.4, and 2.6 nm. A two-dimensional layer-by-layer growth of MgO up to 1 nm is asserted by reflection high-energy electron diffraction (RHEED) intensity oscillations and oscillations of the in-plane lattice parameter. Within this layer-by-layer growth regime, the MgO layer can be considered atomically flat with roughness correlated with the bottom Fe. Above 1 nm thickness, a plastic relaxation

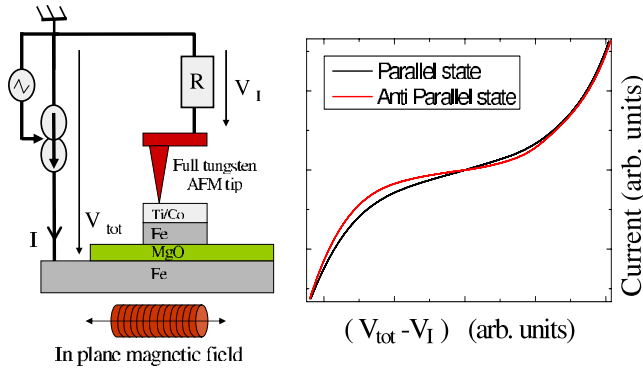


FIG. 1. (Color online) (Left) Schematic of the experimental setup. (Right) Typical $I(V)$ curve obtained for a 2.2-nm-thick MgO layer after averaging 100 measurements.

occurs leading to increased top surface roughness of the MgO. The second magnetic electrode is a bilayer composed of a 10-nm-thick Fe layer, epitaxially grown on the top of the MgO barrier and annealed at 380 °C for 10 min, which is magnetically hardened by a 20-nm-thick Co layer. As we consider the electronic structure, the Fe/MgO/Fe stack is expected to be symmetric with bulk lattice parameters of the two Fe layers. However, the roughness level and the density of defects (i.e., dislocations) of the two interfaces are different. This leads to a structural asymmetry of the stack occurring mainly at the interfaces. Finally, the stack was capped with a Pd(10 nm)/Au(10 nm) bilayer providing large conductivity and preventing *ex situ* oxidation.

Rectangular dots have been defined into the top Fe layer; Titanium dots are first fabricated by e-beam lithography and lift-off process. These dots are then transferred into the magnetic layer by ion-beam etching. The etching is stopped into the MgO tunnel barrier using secondary ion mass spectrometer detection. Shortcuts in the MgO barrier due to possible metallic depositions during the etching are then avoided. The dots are electrically connected by a full metallic tungsten atomic force microscopy (AFM) tip. A schematic of the experimental setup is shown in Fig. 1. A voltage-to-current converter delivers a current whose shape is defined by a function generator. Two different experiments are then performed. The $R(H)$ characteristics are obtained by applying a constant current and an alternative magnetic field H . The $I(V)$ characteristics are obtained with a constant applied magnetic field and an alternative current (20 Hz). The measurement performed during 5 s gives 100 $I(V)$ characteristics. This allows us to check the reproducibility of the measurement. $I(V)$ curves presented in this Brief Report as well as their derivatives are obtained by averaging these 100 characteristics.

A spectroscopy of the DOS is obtained by computing the first derivative of the current with respect to the voltage. A typical $\frac{dI}{dV}(V)$ curve is shown in Fig. 2 for a 2.6-nm-thick MgO barrier. For this sample, a TMR of 80% at zero bias was deduced from the $I(V)$ measurements. In order to highlight any features in the $\frac{dI}{dV}$ curve, we report in the inset the second derivative $|\frac{d^2I}{dV^2}|$ (Fig. 2). Two peaks appear for positive bias at +0.2 and +1.1 V in the antiparallel magnetization state. In

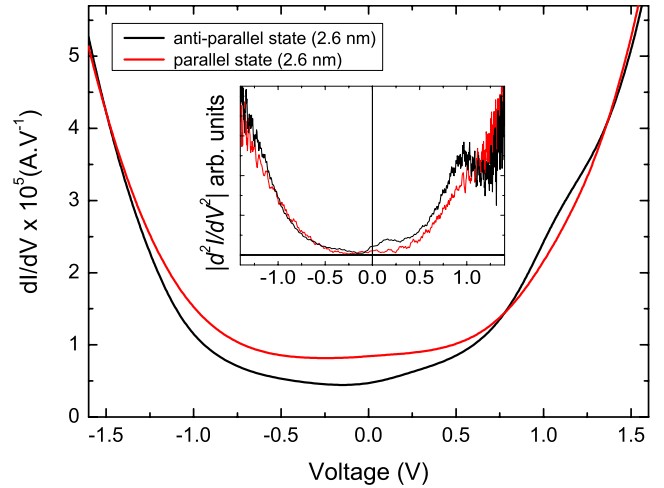


FIG. 2. (Color online) $\frac{dI}{dV}(V)$ for the parallel and the antiparallel Fe magnetization configurations for a 2.6-nm-thick MgO tunnel barrier. Inset: $|\frac{d^2I}{dV^2}(V)|$ for the same states. The peaks at 0.2 and 1.1 V for the antiparallel state are not observed for the parallel state.

this state, for a negative voltage bias, only one small anomaly is hardly observed at -0.2 V. In the parallel state obtained under 0.8 T, no peak appears. The $I(V)$ characteristics for the antiparallel state were measured (Fig. 3) for 2.6-, 2.4-, and 2.2-Å-thick MgO barriers. The amplitudes of the two peaks increase as the thickness of MgO decreases. In order to compare the different $I(V)$ curves, we show in Fig. 4 the evolution of $\delta i(V) = \frac{d(I_{ap} - I_p)}{dV}(V)$, where I_{ap} (I_p) is the current for the antiparallel magnetization state (parallel magnetization state). By multiplying each curve by a constant, they superimpose (inset of Fig. 4). Thus neither the voltage positions of the peaks nor their widths are modified as the MgO thickness is decreased. While the peak located at +0.2 V has been attributed to the IRS at the bottom interface in a tunnel junction with a 3-nm-thick MgO barrier,¹¹ no study as a function of MgO thickness of this IRS or the evidence of a possible second IRS has been shown up to now.

The Fe(001) surface electronic states have already been studied at the Fe(001)/vacuum interface.^{17,18} In Ref. 18, the

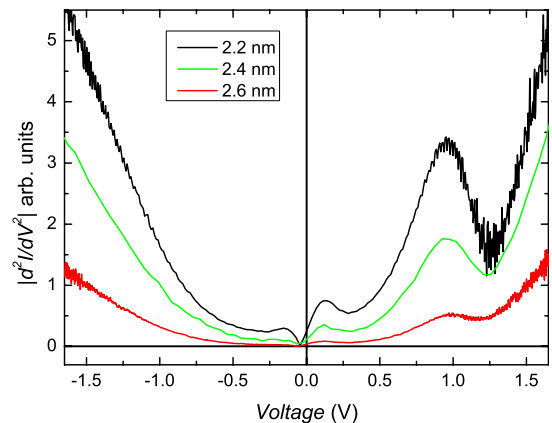


FIG. 3. (Color online) $|\frac{d^2I}{dV^2}(V)|$ for the antiparallel configuration for different MgO thicknesses. The amplitudes of the two peaks increase as the MgO thickness decreases.

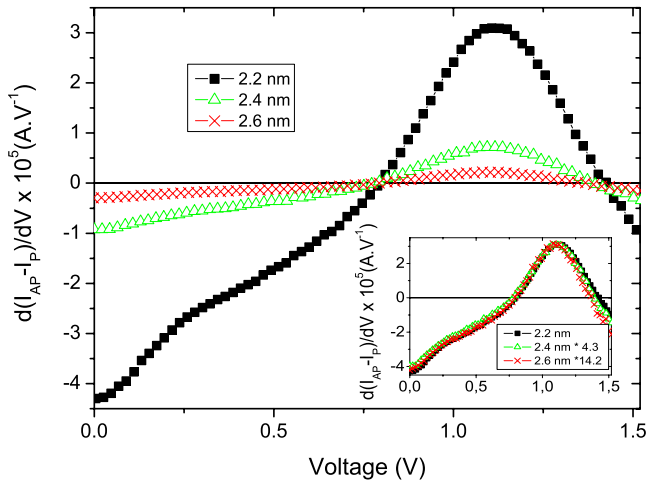


FIG. 4. (Color online) Difference between the differential conductivities in the antiparallel and parallel states, $\delta i(V) = \frac{d(I_{AP} - I_P)}{dV}(V)$, for different MgO thicknesses: 2.2, 2.4, and 2.6 nm. Inset: the 2.4 and 2.6 nm curves have been, respectively, multiplied by attenuation coefficients equal to 4.3 and 14.2. All the curves superimposed showing that neither their position nor their widths are dependent on the MgO thickness.

presence of two surface states above the Fermi level has been predicted for the minority electrons between the $\bar{\Gamma}$ and \bar{X} points: one starting for $k_{\parallel}=0$ at 0.2 eV and the other at 1.5 eV. At the Fe(100)/MgO(100) interface, such states are predicated to exist in the energy gap of the minority Δ_1 symmetry states.^{2,16} Through a coupling with Fe(100) bulk states, they become IRS and available for the transport. At the Fermi level, this state is only available for $k_{\parallel} \neq 0$ while it is situated above the Fermi level around 0.2 eV for $k_{\parallel}=0$. Moreover, this IRS has been theoretically predicted to be very sensitive to interface roughness.²¹ In an “as deposited” Fe/MgO/Fe stack, Tong *et al.*¹⁹ could not observe this IRS and attributed their failure to a too rough interface. Annealing the bottom Fe layer of their epitaxial Fe/MgO/Fe has been shown²² to improve the flatness of the bottom Fe/MgO interface: roughness less than 0.3 nm and atomically flat terraces with size >100 nm. By current perpendicular to plane transport measurements, they have observed the IRS around 0.2 eV at the bottom interface¹¹ on their MTJ stack with a 3-nm-thick MgO barrier. In our samples, as shown in Fig. 3, we also observe a net peak at +0.2 V that could be ascribed to this low-energy IRS. The minority IRS of the bottom interface is “scanned” in energy by the majority Δ_1 electrons at Fermi level of the top electrode. However, a similar peak around -0.2 V with a much smaller amplitude can be observed, especially when the MgO thickness is decreased (Fig. 3). This peak is related to the top electrode which is supposed to have a rougher interface with MgO. It could originate either from an IRS, which is less quenched by a smaller roughness (the top MgO roughness decreases by decreasing the MgO thickness) or from the top of the Δ_5 band of the minority electrons. Therefore, the interpretation of the peaks at ± 0.2 V gets ambiguous: both the IRS and the tail of the Δ_5 band would contribute to its presence.

Interestingly, a second more pronounced peak is observed

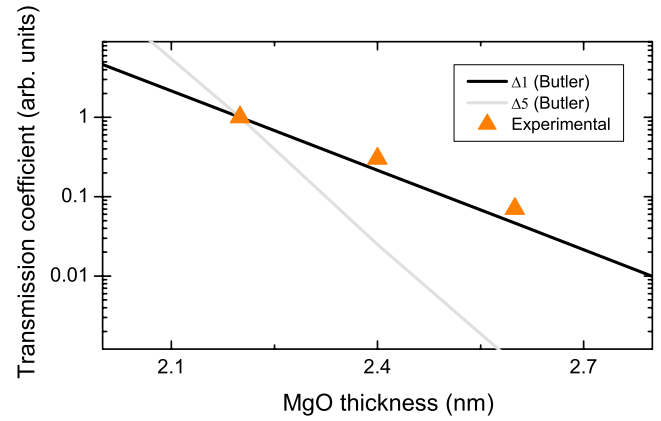


FIG. 5. (Color online) The black (gray) line is the transmission coefficient for $k_{\parallel}=0$ extracted from Ref. 3 for the Δ_1 (Δ_5) symmetry. The small triangles are the transmission coefficient α_t , where $1/\alpha_t$ is the coefficient found for superimposing the 2.4 and 2.6 nm curves to the 2.2 nm one (Fig. 4). For these curves the reference is taken for 2.2 nm.

at +1.1 V (Figs. 2 and 3). Up to now, such a feature at relatively high energy has never been observed by direct tunneling spectroscopy experiments. At negative bias around -1 V, no peak is observed for any MgO thickness, and no feature in the bulk Fe electronic band structure can explain its existence.²³ This clearly demonstrates that it originates from the electronic band structure of the bottom Fe/MgO interface. These surface electronic states are available for the transport; they correspond to an IRS. The DOS of this IRS is so large that around 1 V, the dynamic conductance of the antiparallel state (majority to minority) dominates the conductance of the parallel state (majority to majority) (Figs. 2 and 4). Thus, around this voltage, the dynamic TMR changes sign and its amplitude is increased. This could be an interesting path to follow for applications where sizable TMR values at relatively high voltages are often needed but very difficult to obtain. Furthermore, this result shows that the IRS is preserved by the large period fluctuation level. Supposing that the IRS is a Tamm state with a d character,¹³ it is then much localized with respect to a Shockley state with a sp character.¹² This could explain why the IRS is not destroyed by a roughness with a large fluctuation length.

The low-energy Fe(001) surface state, at 0.2 V, is predicted to have a dominant Δ_1 symmetry in $\bar{\Gamma}(k_{\parallel}=0)$ because it is located in the gap of the Δ_1 bulk band. Similar argument can be used for the higher-energy IRS, at 1.1 V. Anyway, those IRSs should not be purely Δ_1 but a mix of the different symmetries, mainly Δ_1 and Δ_5 , due to the deformation of the orbitals near the interface. Because of this mixing, the surface state becomes an IRS available for conduction as some of the symmetry components (like the Δ_5) couple to bulk conducting states. In order to perform the analysis of the dominant symmetry of the propagating IRS states, we have plotted in Fig. 4 $\delta i(V)$ for the three different MgO thicknesses: 2.2, 2.4, and 2.6 nm. This quantity represents the difference between the transmission in the antiparallel and parallel magnetization configurations. Then, we focused on the IRS density of states. The inset shows the 2.6 and 2.4 nm

curves multiplied by the $1/\alpha_t$ constant found to superimpose with the 2.2 nm one. The increase in the amplitude $\delta i(V)$ with the decrease in the MgO thickness observed in Fig. 3 is due to an increase in the tunneling transmission coefficient through the barrier. Indeed for a given symmetry, the transmission is a convolution of the DOS (bulk and interface) of the bottom Fe layer, the transparency of the barrier, and the DOS of the other electrode. So the variation of the $\delta i(V)$ with MgO thickness depends strongly on the symmetry of the IRS. Figure 5 shows our experimental transmission coefficient as a function of the MgO thickness. On the same figure, the variations with thickness of the theoretical transmission coefficients for $k_{\parallel}=0$ extracted from Ref. 3 for the Δ_1 and the Δ_5 symmetries have been drawn for comparison. For all these plots, the reference is taken to 1 for 2.2 nm. The slope of experimental data decay is in good agreement with theo-

retical slope of the Δ_1 transmission coefficient. This supports that the peak at +1.1 V corresponds to an IRS with a dominant Δ_1 symmetry.

In summary, we have observed asymmetric spectroscopic features on the electrical transmission of single-crystal Fe/MgO magnetic tunnel junctions. The variation with the voltage sign and with the magnetic configuration of the MTJ stack demonstrates the interfacial origin of these peaks. It allows us to investigate separately the top and the bottom interfaces. Our results show the existence of an IRS at the bottom Fe/MgO interface which even dominates the dynamic conductivity at 1.1 eV. On the other hand, the resonant states are destroyed by roughness at the top interface. Finally, the analysis of the transmission coefficients with MgO barrier thickness compared to theoretical predictions suggests a dominant Δ_1 symmetry of the IRS.

-
- ¹W. J. Gallagher and S. S. P. Parkin, IBM J. Res. Dev. **50**, 333 (2006).
- ²W. H. Butler, X. G. Zhang, T. C. Schulthess, and J. M. MacLaren, Phys. Rev. B **63**, 054416 (2001).
- ³X.-G. Zhang and W. H. Butler, J. Phys.: Condens. Matter **15**, R1603 (2003).
- ⁴J. Mathon and A. Umerski, Phys. Rev. B **63**, 220403 (2001).
- ⁵J. Faure-Vincent, C. Tiusan, C. Bellouard, E. Popova, M. Hehn, F. Montaigne, A. Schuhl, and E. Snoeck, J. Appl. Phys. **93**, 7519 (2003).
- ⁶S. S. P. Parkin, C. Kaiser, A. Panchula, P. M. Rice, B. Hughes, M. Samant, and S. H. Yang, Nat. Mater. **3**, 862 (2004).
- ⁷S. Yuasa, T. Nagahama, A. Fukushima, Y. Suzuki, and K. Ando, Nat. Mater. **3**, 868 (2004).
- ⁸C. Tiusan, F. Greullet, M. Hehn, F. Montaigne, S. Andrieu, and A. Schuhl, J. Phys.: Condens. Matter **19**, 165201 (2007).
- ⁹J. M. De Teresa, A. Barthélémy, A. Fert, J. P. Contour, R. Lyonnet, F. Montaigne, P. Seneor, and A. Vaurès, Phys. Rev. Lett. **82**, 4288 (1999).
- ¹⁰S. Yuasa, T. Katayama, T. Nagahama, A. Fukushima, H. Kubota, Y. Suzuki, and K. Ando, Appl. Phys. Lett. **87**, 2508 (2005).
- ¹¹C. Tiusan, J. Faure-Vincent, C. Bellouard, M. Hehn, E. Jouguet, and A. Schuhl, Phys. Rev. Lett. **93**, 106602 (2004).
- ¹²W. Shockley, Phys. Rev. **56**, 317 (1939).
- ¹³I. Tamm, Phys. Z. Sowjetunion **1**, 733 (1932).
- ¹⁴P. H. Dederichs, P. Mavropoulos, O. Wunnicke, N. Papanikolaou, V. Bellini, R. Zeller, V. Drchal, and J. Kudrnovsky, J. Magn. Magn. Mater. **240**, 108 (2002).
- ¹⁵H. F. Ding, W. Wulfhekel, J. Henk, P. Bruno, and J. Kirschner, Phys. Rev. Lett. **90**, 116603 (2003).
- ¹⁶K. D. Belashchenko, J. Velez, and E. Y. Tsybal, Phys. Rev. B **72**, 140404(R) (2005).
- ¹⁷A. M. Turner and J. L. Erskine, Phys. Rev. B **30**, 6675 (1984).
- ¹⁸J. A. Stroscio, D. T. Pierce, A. Davies, R. J. Celotta, and M. Weinert, Phys. Rev. Lett. **75**, 2960 (1995).
- ¹⁹L.-N. Tong, F. Matthes, M. Muller, C. M. Schneider, and C.-G. Lee, Phys. Rev. B **77**, 064421 (2008).
- ²⁰E. Popova *et al.*, Appl. Phys. Lett. **81**, 1035 (2002).
- ²¹E. Tsybal, K. Belashchenko, J. Velez, S. Jaswala, M. van Schilfgaarde, I. Oleynik, and D. Stewart, Prog. Mater. Sci. **52**, 401 (2007).
- ²²J. Faure-Vincent, C. Tiusan, C. Bellouard, E. Popova, M. Hehn, F. Montaigne, and A. Schuhl, Phys. Rev. Lett. **89**, 107206 (2002).
- ²³J. Callaway and C. S. Wang, Phys. Rev. B **16**, 2095 (1977).